

1           **Regional Hydrological Frequency Analysis at Ungauged Sites with**  
2                                   **Random Forest Regression**

3

4                                   Shitanshu Desai<sup>1,\*</sup>, Taha B. M. J. Ouarda<sup>1\*\*</sup>

5       <sup>1</sup> Canada Research Chair in Statistical Hydro-climatology, Centre Eau-Terre-  
6       Environnement, Institut National de la Recherche Scientifique, INRS-ETE, 490 De la  
7       Couronne, Québec (QC), Canada. G1K 9A9.

8

9       \* Corresponding author: shitanshu.desai@ete.inrs.ca; [situdesai@gmail.com](mailto:situdesai@gmail.com)

10       \*\* Co-corresponding author: taha.ouarda@ete.inrs.ca

11

12

13

14

15

16

17

18

19

20

November 2020

21

22 **ABSTRACT:**

23 Flood quantile estimation at sites with little or no data is important for the adequate  
24 planning and management of water resources. Regional Hydrological Frequency Analysis  
25 (RFA) deals with the estimation of hydrological variables at ungauged sites. Random  
26 Forest (RF) is an ensemble learning technique which uses multiple Classification and  
27 Regression Trees (CART) for classification, regression, and other tasks. The RF technique  
28 is gaining popularity in a number of fields because of its powerful non-linear and non-  
29 parametric nature. In the present study, we investigate the use of Random Forest  
30 Regression (RFR) in the estimation step of RFA based on a case study represented by data  
31 collected from 151 hydrometric stations from the province of Quebec, Canada. RFR is  
32 applied to the whole data set and to homogeneous regions of stations delineated by  
33 canonical correlation analysis (CCA). Using the Out-of-bag error rate feature of RF, the  
34 optimal number of trees for the dataset is calculated. The results of the application of the  
35 CCA based RFR model (CCA-RFR) are compared to results obtained with a number of  
36 other linear and non-linear RFA models. CCA-RFR leads to the best performance in terms  
37 of root mean squared error. The use of CCA to delineate neighborhoods improves  
38 considerably the performance of RFR. RFR is found to be simple to apply and more  
39 efficient than more complex models such as Artificial Neural Network-based models.

40

41 **Keywords:**

42 Random Forest Regression, Canonical Correlation Analysis, Regional Flood Frequency  
43 Analysis, Ungauged basin, Machine Learning, Regional estimation.

44

45 **Highlights:**

- 46       • Random Forest Regression (RFR) is used for regional flood frequency analysis  
47       (RFA).
- 48       • RFR is also combined with Canonical Correlation Analysis (CCA): CCA-RFR.
- 49       • The two techniques are compared to other linear and non-linear RFA models.
- 50       • CCA-RFR leads to the best performance in terms of root mean squared error.
- 51       • RFR is simple to apply and more efficient than more complex models.

52

53 **LIST OF ABBREVIATIONS**

54 RFA : Regioanl Frequency Analysis

55 CCA : Canonical Correlation Analysis

56 ANN : Artificial Neural Network

57 GAM : Generalized Additive Model

58 RF : Random Forest

59 RFR : Random Forest Regression

60 CART : Classification and Regression trees

61 CCA-RFR : Random Forest Regression with Canonical Correlation Analysis

62 OOB : out-of-bag

63 SANN : Single Artificial Neural Network

64 EANN : Ensemble Artificial Neural Network

65 CCA-SANN : Single Artificial Neural Network with Canonical Correlation Analysis

66 CCA-EANN : Ensemble Artificial Neural Network with Canonical Correlation Analysis

67 CCA-GAM : Generalized Additive Model with Canonical Correlation Analysis

68 RMSE : Root mean squared error

69 NASH : Nash Sutcliffe model efficiency criterion

70 RMSEr : Relative Root Mean Squared Error

71 BIAS : Mean Bias

72 BIASr : Relative Mean Bias

73 k-fold CV : K-fold Cross Validation

74 Area : Basin Area

75 MBS : Basin Mean Slope

76 FAL : Fraction of Basin Area Occupied by Lakes

77 AMP : Annual Mean Total Precipitation

78 AMD : Annual Mean Degree-days above 0°

79 q100, q50 and q10 : Specific Flood quantiles corresponding to 100, 50 and 10 year return  
80 periods

81 MDI : Mean Decrease in Impurity

82 **1. Introduction**

83 Floods represent one of the most commonly occurring natural disasters ([Stefanidis and](#)  
84 [Stathis, 2013](#)). Floods cause significant environmental, economic and social damages. In  
85 spite of all flood protection measures being taken, from 1990 to 2013, floods have caused  
86 damages of about 600 billion US dollars and close to 7 million deaths worldwide ([Wang](#)  
87 [et al., 2015](#)). Thus, it is of the utmost importance to adequately predict the characteristics  
88 of such events at all sites.

89

90 However, hydrological information may not be available at certain sites of interest. At these  
91 “ungauged sites”, Regional Frequency Analysis (RFA) can be used to develop estimates  
92 of flood characteristics. RFA allows transfer of information from gauged sites to the  
93 ungauged site of interest. RFA usually consists of two main steps. The first step is the  
94 delineation of homogeneous regions. In this step, sites that are similar according to some  
95 homogeneity criteria are grouped together. The rationale here is that as the sites within a  
96 given homogenous region are similar, information can reasonably be transferred from  
97 gauged to ungauged sites. The second step is the application of a regional estimation model  
98 within each delineated region ([Ouarda, 2013; Wazneh et al., 2015](#)). The regional estimation  
99 models are then trained to establish functional relationships between physio-  
100 meteorological basin characteristics and flow characteristics at ungauged basins.

101

102 Delineation can be done on the basis of geographical proximity, but that does not guarantee  
103 that such regions are homogenous in regards to their hydrologic response. In contrast, “Site  
104 focused” regionalization techniques (also called neighborhood-based techniques) have

105 received much attention due to their effectiveness (Ouarda, 2016; Rahman et al., 2019). In  
106 “Site focused” techniques, each site has a prospective set of catchments which form a  
107 homogenous region for that particular site. One such technique is the Region of Influence  
108 (ROI) approach which identifies sites in a homogeneous region based on the distances in  
109 aS multidimensional space of catchment attributes from the target site to the contributing  
110 catchments. Haddad et al. (2012) showed that the ROI approach leads to more efficient and  
111 accurate flood quantile estimates compared to the fixed regions approach. Another such  
112 technique, Canonical Correlation Analysis (CCA), has been used for delineating  
113 homogenous regions in a number of studies ( See for instance Ouarda et al., 2000; Han et al.,  
114 2020). In the present study, CCA is used to delineate homogenous regions as [Ouarda et al.](#)  
115 [\(2008\)](#) indicated that it leads to superior performances.

116

117 Among the large number of RFA estimation methods proposed in the literature, linear  
118 models and their variants are commonly adopted because of their simplicity and the speed  
119 in which they can be trained as well as deployed. However, hydrological systems are  
120 characterized by complex processes and it is unrealistic to assume a linear relationship  
121 between physio-meteorological basin characteristics and flow characteristics. [Sivakumar](#)  
122 [and Singh \(2012\)](#) showed that the relationship between these variables is characterized by  
123 dominant non-linear relationships. [Pandey and Nguyen \(1999\)](#) and [Grover et al. \(2002\)](#)  
124 showed that non-linear regression models provide better performances for RFA.

125

126 Several non-linear techniques have been proposed in the literature. An Artificial Neural  
127 Network (ANN), a non-linear and a non-parametric approach modelled on the neurons

128 present in the human brain, was used for solving several hydrological problems such as  
129 regional flood frequency analysis, streamflow forecasting, rainfall-runoff modelling, flood  
130 forecasting, etc. ([Aziz et al., 2014](#); [Chokmani et al., 2008](#); [Huo et al., 2012](#); Khalil et al.,  
131 2011; [Kumar et al., 2015](#); Ouarda and Shu, 2009; [Tiwari and Chatterjee, 2018](#)).  
132 Generalized Additive Models (GAM) due to their considerable flexibility, are used in  
133 regional flood frequency analysis, water quality estimation, river discharge modeling, etc.  
134 ([Chebana et al., 2014](#); [Iddrisu et al., 2017](#); [Morton and Henderson, 2008](#); Ouarda et al.,  
135 2018; [Rahman et al., 2017](#)). Other non-linear approaches used RFA include Projection  
136 Pursuit Regression ([Durocher et al. \(2015\)](#)), Non-Linear CCA [Ouali et al. \(2015\)](#), and  
137 Adaptive Neuro-Fuzzy Inference Systems (ANFIS) (Shu and Ouarda, 2008).

138

139 Random Forest (RF), first proposed by [Breiman \(2001\)](#), is one such non-linear and non-  
140 parametric technique. It is a popular technique for classification, regression, variable  
141 selection, outlier detection and variable importance. When random forest is used for the  
142 purpose of function approximation or regression, it is called Random Forest Regression  
143 (RFR) or Regression Forests. In RFR, from a given set of data, multiple samples are  
144 randomly drawn and Classification and Regressions Trees (CART) are built. Eventually,  
145 the results of all such trees are combined and an estimate of target variables is obtained by  
146 averaging the outputs of individual trees.

147

148 A number of studies have been conducted in the field of hydrology using RFs. [Chen et al.](#)  
149 [\(2012\)](#) used RF to build a drought forecast model. [Nguyen et al. \(2015\)](#) used RF to forecast  
150 daily water levels. [Monira et al. \(2010\)](#) and [Taksande and Mohod \(2015\)](#) respectively used

151 RF for daily and monthly rainfall forecasting. [Wang et al. \(2015\)](#) developed a flood hazard  
152 risk assessment model based on RF. RF represents a good alternative to Support Vector  
153 Machines ([Meyer et al., 2003](#); [Verikas et al., 2001](#)) and possesses a number of advantages  
154 including a reasonable amount of tolerance towards noise and outliers, high accuracy in  
155 forecasting and no overfitting problems.

156

157 The aim of the present study is to introduce the RF technique for regional flood quantile  
158 estimation. RFR is used to establish non-linear relationships between physio-  
159 meteorological basin characteristics and flow characteristics, and to estimate flood  
160 characteristics at ungauged sites. RFR is also applied to hydrological neighborhoods  
161 derived using CCA (CCA-RFR) for flood quantile estimation. A comparative analysis is  
162 carried out with several other approaches based on the application to a case study of data  
163 derived from the Province of Quebec, Canada.

164

165 The paper is organized as follows. In section 2, the theoretical background of RFR and  
166 CCA is presented along with the evaluation procedure and brief information about the  
167 models to be compared. The case study is presented in section 3 and the results are  
168 presented and discussed in section 4. Finally, the conclusions and recommendations for  
169 further research are presented in section 5.

170

## 171 **2. Methodology**

### 172 **2.1. Random Forest Regression**

#### 173 **2.1.1. RFR Principle**



174 Random Forest is an ensemble learning technique proposed by [Breiman \(2001\)](#). RF is one  
175 of the most accurate general-purpose learning algorithms. Random Forest has been shown  
176 to give a very good performance while using few computational resources. RF exhibits  
177 great performance improvement over single tree algorithms like CART. It is fast and has  
178 error rates comparable to more traditional and resource intensive algorithms.

179

180 In Random forest for regression, the tree predictors  $h(x, \theta_k)$ ,  $k = 1 \dots K$  take on numerical  
181 values depending on the random vectors  $\{\theta_k\}$  ([Breiman, 2001](#)). It is important to note that  
182  $\{\theta_k\}$  are identically distributed and independent random vectors. The training data is  
183 randomly and independently drawn from a joint distribution of  $(X, Y)$ , where the random  
184 vector  $X$  is the observed input and the random vector  $Y$  is the expected numerical output.  
185 Individual trees are grown using the Classification and Regression Trees (CART)  
186 algorithm. Below is the algorithm for Random forest for regression as presented in [Trevor](#)  
187 [et al. \(2009\)](#).

---

(1) For  $b = 1$  to  $B$ :

(a) Draw a bootstrap sample  $Z^*$  of size  $N$  from training data.

(b) Grow a random-forest tree  $T_b$  to the bootstrapped data by recursively repeating  
the following steps for each terminal node of the tree, until the minimum node size  
 $n_{min}$  is reached.

(i) Select  $m$  variables at random from  $p$  variables.

(ii) Pick the best variable/split-point among the  $m$ .

(iii) Split the node into two daughter nodes.

---

---

(2) *Output the ensemble of trees  $\{T_b\}_1^B$*

- *To make a prediction at a new point  $x$ :*

$$\bar{f}_{rf}^B = \frac{1}{B} \sum_{b=1}^B T_b(x)$$

---

188

189 RFR possesses two important features, out-of-bag error rate, and variable importance.  
190 Generally, we use about two third of the data in a bootstrap sample and the rest one third  
191 are left out. These are known as out-of-bag (OOB) samples. The error estimated on these  
192 left out samples is known as OOB-error rate. OOB error rate can be used for validation  
193 purposes as well as for the calculation of the optimum number of trees required. Variable  
194 importance is a measure of which predictors are most useful for predicting the response  
195 variable. Variable importance can be computed using RF by recording improvements, at  
196 each node in every tree in the forest.

197

198 Another advantage of using RFR is that it possesses an ‘acceptable’ tolerance to noise and  
199 outliers, as the input training sets are drawn by random bootstrap sampling, and as the  
200 nodes to be split are selected randomly. Also, as there is no correlation between individual  
201 trees and as each tree is allowed to grow to its maximum size, there is no overfitting of  
202 data. Consequently, the only parameter to be tuned is the number of trees or estimators.

203

204 **2.1.2 Classification and Regression Trees (CART)**

205 CART decision tree is a binary recursion partitioning scheme which is capable of  
206 processing continuous and nominal attributes for regression and classification. In the  
207 present study, we use CART trees for regression. Regression trees are a nonparametric  
208 regression method that approximates real-valued functions. A regression tree is built using  
209 binary partitioning, where each node is iteratively split into two partitions or branches.  
210 Initially, all input variables are grouped into the same partition. Then mean squared error  
211 (mse) is calculated and a split decision is taken. The split decision is taken based on Greedy  
212 minimization. The split which minimizes the mse is selected and further that node is split  
213 into two off-springs. The splitting rule is then applied to each of the new offsprings. Each  
214 tree is grown to the largest possible extent which aids in better regression accuracy.

215

## 216 **2.2 CCA approach in RFA**

217 This section contains a brief discussion about CCA and its connection to the delineation step of  
218 RFA. Let  $X = \{X_1, X_2 \dots X_r\}$  be a random variable containing basin meteorological and  
219 physiographical variables, for eg. basin area, etc. and  $Y = \{Y_1, Y_2 \dots Y_r\}$  be a random variable  
220 containing basin hydrological variables like flood quantiles.

221

222 Consider linear combinations  $V$  and  $W$  of the variables  $X$  and  $Y$ :

$$223 \quad V = a_1X_1 + a_2X_2 + \dots + a_rX_r = a'X \quad (1)$$

$$224 \quad W = b_1Y_1 + b_2Y_2 + \dots + b_rY_r = b'Y \quad (2)$$

225 where  $a'$  and  $b'$  are transposes of vector  $a$  and  $b$  respectively. CCA enables identifying  
226 vectors  $a$  and  $b$  such that  $corr(V, W)$  is maximum with vectors  $V$  and  $W$  having unit

227 variances. For each basin  $B_k$ , where  $k = 1, 2 \dots K$  from the set  $B$  of basins,  $v_{i,k}$  and  $w_{i,k}$  are  
228 corresponding values of  $V_i$  and  $W_i$ . We have the values of vector  $v_0$  and our aim is to  
229 estimate the unknown vector  $w_0$ , where  $v_0$  and  $w_0$  represent the canonical scores of  
230 physio-meteorological and hydrological variables respectively.

231

232 The approximation of the  $w_0$  vector can be obtained from a  $100(1 - \alpha)\%$  confidence  
233 interval about  $\lambda v_0$  by constituting all the realizations  $w$  of  $W$  where:

$$234 \quad (w - \lambda v_0)'(I_p - \lambda^2)^{-1}(w - \lambda v_0) \leq \chi_{\alpha,p}^2, \quad (3)$$

235 is conditional on  $\chi_{\alpha,p}^2$  being  $P(\chi^2 \leq \chi_{\alpha,p}^2) = 1 - \alpha$ . For more detailed information  
236 concerning the algorithm, the reader is referred to ([Ouarda et al., 2001](#)).

237

### 238 **2.3. Selection of Methods for Comparison**

239 The RFR and CCA-RFR models are used to estimate the 100, 50 and 10-year flood  
240 quantiles. To evaluate the relative performances of these two approaches, they are  
241 compared to the following models:

242

- 243 • Canonical Correlation Analysis-Multiple linear regression model (CCA-MLR) ([Ouarda et](#)  
244 [al., 2001](#)). After selecting the optimal hydrological neighborhoods for each site using CCA  
245 analysis, multiple regression is used for regional flood estimation.

246 • Single Artificial Neural Network (SANN) ([Shu and Burn, 2004](#)). A single ANN is used  
247 to identify a functional relationship between physio-meteorological variables and flood  
248 quantiles.

249 • Ensemble ANN (EANN) ([Shu and Burn, 2004](#)). An ANN ensemble is created by bagging  
250 several single ANNs. This helps in improving the generalization ability of the SANN model.  
251 The final output is generated by taking the mean of the outputs of individual ANNs.

252 • Canonical Kriging Model (CCA-Kriging) ([Chokmani and Ouarda, 2004](#)). The  
253 physiographical space defined by CCA is used by the Kriging model to obtain regional flood  
254 estimates by interpolating data over that physiographic space. This method was shown to  
255 lead to comparable results to the traditional CCA model but is computationally less  
256 complicated.

257 • Single Artificial Neural Network in CCA physiographical space (CCA-SANN) ([Shu and](#)  
258 [Ouarda, 2007](#)). CCA is used to form the canonical physiographical space and then single  
259 ANN is applied to the data to form functional relationships between physiographical  
260 variables and flood quantiles.

261 • Ensemble ANN in CCA physiographical space (CCA-EANN) ([Shu and Ouarda, 2007](#)).  
262 In the CCA-EANN model, each component uses the same configuration as a Single ANN  
263 but the CCA-EANN is trained on bootstrapped sample data and the results are averaged out.

264 • Generalized Additive Model in conjunction with CCA (CCA-GAM) ([Chebana et al.,](#)  
265 [2014](#)). In the CCA-GAM approach, firstly backward stepwise selection is used to select the  
266 variables to be used in the model. Then GAM is applied to the neighborhoods delineated by  
267 CCA.

268

## 269 2.4. Evaluation Metrics

270 The following metrics are used to assess the quality of our regional flood analysis models. They  
271 are NASH (Nash Criterion), RMSE (Root mean squared error), RMSEr (Relative Root Mean  
272 Squared Error), BIAS (Mean Bias) and BIASr (Relative Mean Bias).

273

$$274 \quad NASH = 1 - \frac{\sum_{i=1}^n (o_i - s_i)^2}{\sum_{i=1}^n (o_i - \bar{o})^2} \quad (4)$$

$$275 \quad RMSE = \sqrt{\frac{1}{n} \sum_{i=1}^n (o_i - s_i)^2} \quad (5)$$

$$276 \quad RMSEr = \sqrt{\frac{1}{n} \sum_{i=1}^n \left( \frac{o_i - s_i}{o_i} \right)^2} \quad (6)$$

$$277 \quad BIAS = \frac{1}{n} \sum_{i=1}^n (o_i - s_i) \quad (7)$$

$$278 \quad BIASr = \frac{1}{n} \sum_{i=1}^n \left( \frac{o_i - s_i}{o_i} \right) \quad (8)$$

279

280 where,  $o_i$  is the observed value at site  $i$ ,  $s_i$  is the simulated value using the model for site  
281  $i$ ,  $\bar{o}$  is the mean of observed at-site values and  $n$  is the number of sites.

282

## 283 2.5. Evaluation Procedure

284 K-fold Cross Validation (k-fold CV) is used as the model validation technique in this work.

285 In k-fold CV the data is split into  $k$  small and equal sets. A model is trained using  $k - 1$

286 folds as training data and then the model is validated using the remaining data. The

287 performance thus reported by k-fold CV is the mean of the values computed in the loop.

288

289 The reason for using k-fold CV in the present study is that models trained with k-fold CV  
290 have lower variance than models trained with the jackknife validation procedure. In  
291 jackknife validation, there is more overlap between training folds as only one sample is  
292 omitted which means that almost the entire dataset is used for training. While in k-fold CV  
293 there is less overlap between training folds and thus it leads to smaller variability.  
294 Therefore, results obtained with jackknife might be better but the results obtained using k-  
295 fold CV are more robust.

296

### 297 **3. Case Study**

298 The dataset used in the present study consists of 151 hydrometric stations located in the  
299 southern part of the province of Quebec (between 45° and 55°N), Canada. The stations are  
300 operated by the Ministry of Environment of Quebec. The adopted dataset has been used in  
301 a number of previous RFA studies ([Chebana and Ouarda, 2008](#); [Shu and Ouarda, 2007](#))  
302 making it convenient for comparison of the results with those obtained with other  
303 methodologies.

304

305 On the basis of the work of [Chokmani and Ouarda \(2004\)](#) with the same database, a total  
306 of five physio-meteorological variables are selected, of which three are physiographical  
307 and two are meteorological variables. These variables are the basin area (Area), the mean  
308 basin slope (MBS), the fraction of basin area occupied by lakes (FAL), the annual mean  
309 total precipitation (AMP) and the annual mean degree-days above 0° (AMD), respectively.

310 A number of statistics of these data, like the minimum, mean, maximum and standard  
311 deviation are presented in table 1.

312

313 The database compiled by ([Kouider et al., 2002](#)) is used to extract at-site flood estimates  
314 for all of the 151 gauging stations in the study area. The most appropriate statistical  
315 distribution is used to get flood quantile estimates for each site by fitting the distribution to  
316 observed flood data. To avoid negative scale effects, specific quantiles (quantiles divided  
317 by basin areas) are used. The 100-year, 50-year, and 10-year quantiles (q100, q50, and q10  
318 respectively) are the three specific flood quantiles used in the present study.

319

320 The reader is directed to ([Shu and Ouarda, 2007](#)) for more details concerning the dataset,  
321 such as scatter plots of basins in canonical space and geographical location of stations, to  
322 avoid redundancy. According to the recommendations of [Shu and Ouarda \(2007\)](#), the  
323 logarithmic transformation is applied to the variables q10, q50, q100, Area, MBS, AMP  
324 and AMD and a square root transformation is applied to FAL.

325

#### 326 **4. Results**

327 In the present study, Scikit-learn module of Python is used to obtain the results ([Pedregosa  
328 et al., 2011](#)). In RF the size of the dataset, the number of trees (n\_estimators) and the  
329 number of variables at each split have a huge impact on the error rate. According to  
330 [Breiman \(2001\)](#), the number of variables at each split should be taken as the square root of



331 the total number of variables, i.e. 2 in this study. As the size of the dataset is not a tunable  
332 parameter, only the number of trees is tuned in this study.

333

334 Figure 1 illustrates that the OOB error rate decreases as the number of trees increases. At  
335 around 30 trees the value levels off and there is almost no improvement after this point by  
336 increasing the number of trees. Therefore, the number of trees is fixed at 30 for the present  
337 study. It is also important to note that all the trees were allowed to grow to the maximum  
338 extent without pruning.

339

340 The results of the application of the two models RFR and CCA-RFR along with the models  
341 described in Section 0 to the dataset described in Section 0 are illustrated in Table 2. The  
342 bold font describes the best approach for that particular flood quantile and the particular  
343 evaluation metric. Results indicate that CCA-RFR either outperforms or is comparable to  
344 other models in all the metrics except the NASH criterion. Also, CCA-RFR outperforms  
345 RFR in every metric other than NASH.

346

347 Figure 2 illustrates the relative errors associated with quantiles q50 estimated using RFR  
348 and CCA-RFR. Figure 2 indicates that CCA-RFR performs better than RFR for large  
349 basins, while RFR outperforms CCA-RFR for very small basins. These smaller basins are  
350 associated with larger specific quantiles. Therefore we can attribute the low NASH scores  
351 associated to CCA-RFR to these smaller sites Similarly, according to [McCuen et al. \(2006\)](#),  
352 the NASH criterion is sensitive to a number of factors including sample size and outliers.

353 In CCA-RFR, as only the stations in the hydrological neighborhoods are considered for the  
354 prediction and training, the sample size is considerably smaller than the complete original  
355 dataset. Also, the NASH criterion is heavily influenced by the model used ([Schaefli and](#)  
356 [Gupta, 2007](#)). RFR provides a reasonable tolerance to outliers which can be seen in the  
357 RFR NASH values. However, as we use just the neighborhoods for CCA-RFR, the sample  
358 size is small and thus outliers have more effect than in the basic RFR model which leads  
359 to lower NASH values.

360

361 Although we have low values for the NASH criterion for both RFR and CCA-RFR in  
362 comparison to other models, we can observe that CCA-RFR leads to the best RMSE and  
363 RMSEr values among all the models studied in this work. RMSE provides an evaluation  
364 of prediction accuracy in the absolute scale while RMSEr does the same in relative terms.  
365 CCA based RFR provides better generalization ability than the basic RFR model. As RFRs  
366 are nonparametric data-driven approaches, they have limited scope for extrapolation  
367 beyond the observed data. Therefore, the combination of RFR along with CCA, a  
368 parametric model helps the performance of RFR. Consequently, even though the NASH  
369 value for CCA-RFR is lower than other models the prediction accuracy is not compromised  
370 and is rather improved.

371

372 The BIAS and BIASr are evaluation criteria used to determine whether the model  
373 overestimates or underestimates the various quantiles. In general, CCA-RFR has the lowest  
374 BIAS of all the models considered and BIASr is also comparable with CCA-EANN and

375 CCA-GAM which have the best BIASr value. It is also important to point out that, in terms  
376 of BIAS, CCA-RFR overestimates flood quantiles while RFR underestimates them.  
377 However, when BIASr is used, all the models underestimate the flood quantiles.

378

379 Overall, it can be concluded that applying RFR to CCA delineated neighborhoods improves  
380 the results in comparison to RFR applied to the whole set of stations. This is consistent  
381 with the results of previous studies, such as [Chokmani and Ouarda \(2004\)](#) and [Shu and](#)  
382 [Ouarda \(2007\)](#), which indicated that applying other estimation techniques to CCA  
383 delineated neighborhoods leads to better performances for the estimation of flood quantiles  
384 than their application to the whole set of stations in the database.

385

386 The scatter plots of regional estimates using RFR and CCA-RFR are shown in Figure 3  
387 and Figure 4, respectively. As would be expected, we observe that the estimation error and  
388 bias are positively correlated with the return period. With the increase in return periods,  
389 bias and estimation error increase simultaneously. Also, the low NASH scores can be  
390 explained by high variation as seen in Figure 4. It is clear from the results that all models  
391 underestimate flood quantiles at sites with higher specific quantiles. These sites can be  
392 associated with smaller basins which have large specific quantiles ([Shu and Ouarda, 2007](#)).

393

394 An additional experiment is conducted to identify the importance of individual predictor  
395 variables for flood quantile estimation. In the python implementation of RFR, “Mean  
396 decrease in Impurity (MDI)” or “Gini importance” is used to calculate the importance of

397 each variable on the accuracy of the model. MDI is defined as “total decrease in node  
398 impurity averaged over all the trees. Node impurity is weighted by the probability of  
399 reaching that node (which is approximated by the proportion of sample reaching that  
400 node)”([Brieman et al., 1984](#)). The results are illustrated in Table 3. Basin Area (Area) is  
401 shown to be by far the most important physio-meteorological variable. Annual mean total  
402 precipitation (AMP) and Annual mean degree days over 0° C (AMD) are distant second  
403 and third, respectively. Mean Basin Slope (MBS) is fourth while the Fraction of Area  
404 covered by lakes (FAL) is the least important of all physio-meteorological variables.

405

## 406 **5. Conclusions**

407 RF has been commonly used in gene classification, banking, medicine, and E-commerce.  
408 However, so far it has not found much application in the field of hydrology and especially  
409 in RFA. Most common studies in RFA establish linear relationships between physio-  
410 meteorological variables and flood quantiles. However, these models do not generally  
411 explain the complex relationships between the response variable and the explanatory  
412 variables. Random forest, a non-linear and a non-parametric data-driven approach, is one  
413 such technique which has shown good performances in other fields in explaining such  
414 complex relationships. This method is very easy to apply in practice as it does not require  
415 specific subjective choices by the user. The purpose of this study is to first introduce RFR  
416 in RFA and then apply RFR to neighborhoods delineated by CCA.

417

418 The number of trees in the RF for this study was fixed at 30. Also, all the trees were allowed  
419 to grow to their maximum potential without pruning. The comparison with other models

420 indicates that, although CCA-RFR has a lower NASH score, it is more accurate than the  
421 other models. RFR is particularly more advantageous because of its low computational cost  
422 and high prediction quality. The results further indicate that the Random Forest, when used  
423 in conjunction with CCA, provides more robust and accurate results.

424

425 The research presented in this work is based on the introduction of the RF approach to  
426 RFA. The use of Extremely Randomized Trees and other variants of RF in RFA should  
427 also be attempted in the future. Future research activities should also focus on the use of  
428 RF in conjunction with other delineation techniques such as the Region of Influence  
429 approach, statistical depth functions, or projection pursuit regression. The effectiveness of  
430 the same techniques should also be investigated in the future using other data sets from  
431 different climates and different parts of the world to check the generality of the results  
432 obtained in this study. The efficiency of the technique should especially be examined for  
433 case studies with a higher level of heterogeneity in the physiographical variables. Future  
434 efforts should also investigate the use of the RF approach in the case of partially gauged  
435 sites and in the context of the use of procedures for the combination of local and regional  
436 information (see Seidou et al., 2006, for instance). The extension of the approach to the  
437 nonstationary case and for other hydrological variables such as low flows or suspended  
438 sediments should also be considered.

439

440 **6. Acknowledgments.** Financial support for this study was graciously provided by the  
441 Natural Sciences and Engineering Research Council (NSERC) of Canada. The authors

442 would like to thank the Ministry of Sustainable Development, Environment, and Fight  
443 Against Climate Change of the Province of Quebec (MDDELCC) for the employed  
444 datasets. The authors would like to thank the Editor, Prof. Andras Bardossy, the Associate  
445 Editor, Prof. Félix Francés, and two anonymous reviewers for all their efforts and for their  
446 comments which helped improve the quality of the manuscript.

447 **7. References**

448

449 Aziz, K., Rahman, A., Fang, G., Shrestha, S., 2014. Application of artificial neural networks in

450 regional flood frequency analysis: a case study for Australia. *Stochastic Environmental*

451 *Research and Risk Assessment*, 28(3): 541-554. DOI:10.1007/s00477-013-0771-5

452 Breiman, L., 2001. Random forests. *Machine Learning*, 45(1): 5-32.

453 DOI:10.1023/a:1010933404324

454 Brieman, L., Friedman, J., Olshen, R., Stone, C., 1984. *Classification and Regression Trees*.

455 Wadsworth. Inc, Pacific Grove, CA.

456 Chebana, F., Charron, C., Ouarda, T.B.M.J., Martel, B., 2014. Regional Frequency Analysis at

457 Ungauged Sites with the Generalized Additive Model. *Journal of Hydrometeorology*, 15(6):

458 2418-2428. DOI:10.1175/jhm-d-14-0060.1

459 Chebana, F., Ouarda, T.B., 2008. Depth and homogeneity in regional flood frequency analysis.

460 *Water resources research*, 44(11).

461 Chen, J., Li, M., Wang, W., 2012. Statistical uncertainty estimation using random forests and its

462 application to drought forecast. *Mathematical Problems in Engineering*, 2012.

463 Chokmani, K., Ouarda, T.B.M.J., Hamilton, S., Ghedira, M.H., Gingras, H., 2008. Comparison of

464 ice-affected streamflow estimates computed using artificial neural networks and multiple

465 regression techniques. *Journal of Hydrology*, 349(3-4): 383-396.

466 DOI:10.1016/j.jhydrol.2007.11.024

467 Chokmani, K., Ouarda, T.B.M.J., 2004. Physiographical space-based kriging for regional flood

468 frequency estimation at ungauged sites. *Water Resources Research*, 40(12).

469 DOI:10.1029/2003wr002983

470 Durocher, M., Chebana, F., Ouarda, T.B.M.J., 2015. A Nonlinear Approach to Regional Flood

471 Frequency Analysis Using Projection Pursuit Regression. *Journal of Hydrometeorology*,

472 16(4): 1561-1574. DOI:10.1175/jhm-d-14-0227.1

473 Grover, P.L., Burn, D.H., Cunderlik, J.M., 2002. A comparison of index flood estimation  
474 procedures for ungauged catchments. *Canadian Journal of Civil Engineering*, 29(5): 734-741.  
475 DOI:10.1139/102-065

476 Han, X., Ouarda, T.B.M.J., Rahman, A., Haddad, K., Mehrotra, R., Sharma, A., 2020. A Network  
477 Approach for Delineating Homogeneous Regions in Regional Flood Frequency Analysis.  
478 *Water Resources Research*, 56(3): e2019WR025910. DOI:10.1029/2019wr025910

479 Haddad, K., Rahman, A., 2012. Regional flood frequency analysis in eastern Australia: Bayesian  
480 GLS regression-based methods within fixed region and ROI framework – Quantile  
481 Regression vs. Parameter Regression Technique. *Journal of Hydrology*, 430-431: 142-161.  
482 DOI:10.1016/j.jhydrol.2012.02.012

483 Huo, Z., Feng, S., Kang, S., Huang, G., Wang, F., Guo, P., 2012. Integrated neural networks for  
484 monthly river flow estimation in arid inland basin of Northwest China. *Journal of Hydrology*,  
485 420-421: 159-170. DOI:10.1016/j.jhydrol.2011.11.054

486 Iddrisu, W.A., Nokoe, K.S., Luguterah, A., Antwi, E.O., 2017. Generalized Additive Mixed  
487 Modelling of River Discharge in the Black Volta River. *Open Journal of Statistics*, 07(04):  
488 621-632. DOI:10.4236/ojs.2017.74043

489 Khalil, B., Ouarda, T.B.M.J., St-Hilaire, A., 2011. Estimation of water quality characteristics at  
490 ungauged sites using artificial neural networks and canonical correlation analysis. *Journal of*  
491 *Hydrology*, 405(3–4): 277-287. DOI:10.1016/j.jhydrol.2011.05.024

492 Kouider, A., Gingras, H., Ouarda, T., Ristic-Rudolf, Z., Bobée, B., 2002. Analyse fréquentielle  
493 locale et régionale et cartographie des crues au Québec. Research report (R619). INRS-Eau,  
494 Terre et Environnement, Québec.

495 Kumar, R., Goel, N.K., Chatterjee, C., Nayak, P.C., 2015. Regional Flood Frequency Analysis  
496 using Soft Computing Techniques. *Water Resources Management*, 29(6): 1965-1978.  
497 DOI:10.1007/s11269-015-0922-1



498 McCuen, R.H., Knight, Z., Cutter, A.G., 2006. Evaluation of the Nash–Sutcliffe efficiency index.  
499 Journal of Hydrologic Engineering, 11(6): 597-602. DOI:doi:10.1061/(ASCE)1084-  
500 0699(2006)11:6(597)

501 Meyer, D., Leisch, F., Hornik, K., 2003. The support vector machine under test. Neurocomputing,  
502 55(1-2): 169-186. DOI:10.1016/s0925-2312(03)00431-4

503 Monira, S.S., Faisal, Z.M., Hirose, H., 2010. Comparison of artificially intelligent methods in  
504 short term rainfall forecast, Computer and Information Technology (ICCIT), 2010 13th  
505 International Conference on. IEEE, pp. 39-44. DOI:10.1109/ICCITECHN.2010.5723826

506 Morton, R., Henderson, B.L., 2008. Estimation of nonlinear trends in water quality: An improved  
507 approach using generalized additive models. Water Resources Research, 44(7).  
508 DOI:10.1029/2007wr006191

509 Nguyen, T.-T., Huu, Q.N., Li, M.J., 2015. Forecasting time series water levels on Mekong river  
510 using machine learning models, Knowledge and Systems Engineering (KSE), 2015 Seventh  
511 International Conference on. IEEE, pp. 292-297. DOI:10.1109/KSE.2015.53

512 Ouali, D., Chebana, F., Ouarda, T.B.M.J., 2015. Non-linear canonical correlation analysis in  
513 regional frequency analysis. Stochastic Environmental Research and Risk Assessment, 30(2):  
514 449-462. DOI:10.1007/s00477-015-1092-7

515 Ouarda, T.B.M.J., 2013. Hydrological Frequency Analysis, Regional, Encyclopedia of  
516 Environmetrics. DOI:10.1002/9780470057339.vnn043

517 Ouarda, T.B.M.J., 2016. Regional flood frequency modeling, Chap. 77, Chow’s Handbook of  
518 Applied Hydrology, 2nd Edn., edited by Singh, V. P. Mc-Graw Hill, New York, pp. 77.1–  
519 77.8, ISBN 978-0-07-183509-1

520 Ouarda, T.B.M.J., Ba, K.M., Diaz-Delgado, C., Carsteanu, A., Chokmani, K., Gingras, H.,  
521 Quentin, E., Trujillo, E., Bobee, B., 2008. Intercomparison of regional flood frequency  
522 estimation methods at ungauged sites for a Mexican case study. Journal of Hydrology, 348(1-  
523 2): 40-58. DOI:10.1016/j.jhydrol.2007.09.031

524 Ouarda, T.B.M.J., Charron, C., Hundecha, Y., Saint-Hilaire, A., Chebana, F., 2018. Introduction  
525 of the GAM model for regional low-flow frequency analysis at ungauged basins and  
526 comparison with commonly used approaches. *Environmental Modelling & Software*, 109:  
527 256-271. DOI:10.1016/j.envsoft.2018.08.031

528 Ouarda, T.B.M.J., Girard, C., Cavadias, G.S., Bobée, B., 2001. Regional flood frequency  
529 estimation with canonical correlation analysis. *Journal of Hydrology*, 254(1-4): 157-173.  
530 DOI:10.1016/S0022-1694(01)00488-7

531 Ouarda, T.B.M.J., Haché, M., Bruneau, P., Bobée, B., 2000. Regional flood peak and volume  
532 estimation in northern Canadian basin. *Journal of cold regions engineering*, 14(4): 176-191.  
533 DOI:10.1061/(ASCE)0887-381X(2000)14:4(176)

534 Ouarda, T.B.M.J., Shu, C., 2009. Regional low-flow frequency analysis using single and  
535 ensemble artificial neural networks. *Water Resources Research*, 45(11): W11428.  
536 DOI:10.1029/2008wr007196

537 Pandey, G., Nguyen, V.-T.-V., 1999. A comparative study of regression based methods in  
538 regional flood frequency analysis. *Journal of Hydrology*, 225(1-2): 92-101.  
539 DOI:10.1016/S0022-1694(99)00135-3

540 Pedregosa, F., Varoquaux, G., Gramfort, A., Michel, V., Thirion, B., Grisel, O., Blondel, M.,  
541 Prettenhofer, P., Weiss, R., Dubourg, V., 2011. Scikit-learn: Machine learning in Python.  
542 *Journal of machine learning research*, 12: 2825-2830.

543 Rahman, A., Charron, C., Ouarda, T.B.M.J., Chebana, F., 2017. Development of regional flood  
544 frequency analysis techniques using generalized additive models for Australia. *Stochastic  
545 Environmental Research and Risk Assessment*, 32(1): 123-139. DOI:10.1007/s00477-017-  
546 1384-1

547 Rahman, A., Haddad, K., Kuczera, G., Weinmann, E., 2019. Regional flood methods. *Australian  
548 Rainfall and Runoff: A Guide To Flood Estimation*. Book 3, Peak Flow Estimation: 105-146.

549 Schaeffli, B., Gupta, H.V., 2007. Do Nash values have value? *Hydrological Processes*, 21(15):  
550 2075-2080. DOI:10.1002/hyp.6825

551 Seidou, O., Ouarda, T.B.M.J., Barbet, M., Bruneau, P., Bobée, B., 2006. A parametric Bayesian  
552 combination of local and regional information in flood frequency analysis. *Water Resources*  
553 *Research*, 42(11): W11408. DOI:10.1029/2005wr004397

554 Shu, C., Burn, D.H., 2004. Artificial neural network ensembles and their application in pooled  
555 flood frequency analysis. *Water Resources Research*, 40(9). DOI:10.1029/2003wr002816

556 Shu, C., Ouarda, T.B.M.J., 2007. Flood frequency analysis at ungauged sites using artificial  
557 neural networks in canonical correlation analysis physiographic space. *Water Resources*  
558 *Research*, 43(7). DOI:10.1029/2006wr005142

559 Shu, C., Ouarda, T.B.M.J., 2008. Regional flood frequency analysis at ungauged sites using the  
560 adaptive neuro-fuzzy inference system. *Journal of Hydrology*, 349(1-2): 31-43.  
561 DOI:10.1016/j.jhydrol.2007.10.050

562 Sivakumar, B., Singh, V.P., 2012. Hydrologic system complexity and nonlinear dynamic  
563 concepts for a catchment classification framework. *Hydrology and Earth System Sciences*,  
564 16(11): 4119-4131. DOI:10.5194/hess-16-4119-2012

565 Stefanidis, S., Stathis, D., 2013. Assessment of flood hazard based on natural and anthropogenic  
566 factors using analytic hierarchy process (AHP). *Natural Hazards*, 68(2): 569-585.  
567 DOI:10.1007/s11069-013-0639-5

568 Taksande, A.A., Mohod, P., 2015. Applications of data mining in weather forecasting using  
569 frequent pattern growth algorithm. *IJSR*, 4(6): 3048-51.

570 Tiwari, M.K., Chatterjee, C., 2018. Flood Forecasting and Uncertainty Assessment Using  
571 Wavelet- and Bootstrap-Based Neural Networks, *Handbook of Research on Predictive*  
572 *Modeling and Optimization Methods in Science and Engineering*. *Advances in*  
573 *Computational Intelligence and Robotics*, pp. 74-93. DOI:10.4018/978-1-5225-4766-2.ch004

574 Hastie, T., Tibshirani, R., Friedman, J., 2009. The elements of statistical learning: data mining,  
575 inference, and prediction. Springer, New York, NY.

576 Verikas, A., Gelzinis, A., Malmqvist, K., 2001. Using unlabelled data to train a multilayer  
577 perceptron. *Neural Processing Letters*, 14(3): 179-201. DOI:10.1023/A:1012707515770

578 Wang, Z., Lai, C., Chen, X., Yang, B., Zhao, S., Bai, X., 2015. Flood hazard risk assessment  
579 model based on random forest. *Journal of Hydrology*, 527: 1130-1141.  
580 DOI:10.1016/j.jhydrol.2015.06.008

581 Wazneh, H., Chebana, F., Ouarda, T.B.M.J., 2015. Delineation of homogeneous regions for  
582 regional frequency analysis using statistical depth function. *Journal of Hydrology*, 521: 232-  
583 244. DOI:10.1016/j.jhydrol.2014.11.068

584

585

586 **LIST OF TABLES AND FIGURE CAPTIONS**

587

588 Table 1 : Descriptive Statistics of physio-meterological and Hydrological Variables.

589 Table 2: NASH, RMSE, RMSEr, BIAS and BIASr values for all the models. Best values  
590 for each quantile for the corresponding metrics are marked in bold.

591 Table 3: Feature Importance of Five Input Variables used for Specific Flood Quantile  
592 Estimation.

593

594 Figure 1: Number of trees (n\_estimators) vs OOB error rate for 10, 50 and 100-year flood  
595 quantiles.

596 Figure 2: Relative errors associated with at-site quantile q50 calculated using RFR and CCA-RFR  
597 (the sites are ordered according to their area)

598 Figure 3: A) q10, B) q50 and C) q100 estimation using RFR approach.

599 Figure 4: A) q10, B) q50 and C) q100 estimation using CCA-RFR approach.

600

601 Table 1: Descriptive Statistics of physio-meterological and Hydrological Variables.

Variables	Minimum	Mean	Maximum	Standard deviation
q10 (m <sup>3</sup> /s.km <sup>2</sup> )	0.03	0.31	0.94	0.20
q50 (m <sup>3</sup> /s.km <sup>2</sup> )	0.03	0.28	0.77	0.18
q100 (m <sup>3</sup> /s.km <sup>2</sup> )	0.03	0.22	0.53	0.13
Area (km <sup>2</sup> )	208	6255	96600	11716
MBS (%)	0.96	2.43	6.81	0.99
FAL (%)	0.00	7.72	47.00	7.99
AMP (mm)	646	988	1534	154
AMD (degree day)	8589	16346	29631	5382

602

603

604

605

606

607

608

609

610

611

612

613

614 Table 2: NASH, RMSE, RMSEr, BIAS and BIASr values for all models. Best values for each  
 615 quantile for the corresponding metrics are marked in bold.

	Hydrological Variables	CCA- SANN	CCA- EANN	CCA- Kriging	CCA- MLR	SANN	EANN	CCA- GAM	RFR	CCA- RFR
NASH	q10	0.82	<b>0.84</b>	0.78	0.78	0.75	0.78	0.82	0.721	0.577
	q50	0.78	<b>0.8</b>	0.72	0.72	0.69	0.72	0.76	0.657	0.532
	q100	0.77	<b>0.78</b>	0.7	0.68	0.66	0.69	0.67	0.644	0.507
RMSE	q10	0.053	0.05	0.05	0.059	0.06	0.058	0.054	0.063	<b>0.049</b>
	q50	0.082	0.079	0.093	0.094	0.098	0.093	0.087	0.089	<b>0.07</b>
	q100	0.095	0.093	0.11	0.112	0.115	0.109	0.115	0.099	<b>0.08</b>
RMSEr	q10	38	37	51	43	47	44	33.7	80.74	<b>29.44</b>
	q50	44	43	64	49	55	53	43.5	93.39	<b>33.27</b>
	q100	46	45	70	51	64	60	37.0	96.45	<b>35.02</b>
BIAS	q10	0.006	0.005	-0.004	<b>0.001</b>	0.006	0.004	0.009	-0.0013	0.002
	q50	0.009	0.009	-0.007	0.005	0.01	0.009	<b>-0.003</b>	-0.0073	<b>0.003</b>
	q100	0.013	0.012	-0.008	0.007	0.015	0.013	0.043	-0.019	<b>0.004</b>
BIASr	q10	-5	-5	-16	-9	-7	-7	<b>-3.5</b>	-21.12	-6.64
	q50	-7	<b>-5</b>	-21	-11	-8	-8	-11.4	-25.97	-8.14
	q100	-7	-6	-23	-11	-11	-10	<b>3.4</b>	-27.85	-8.89

616

617

618

619

620 Table 3: Feature Importance of Five Input Variables used for Specific Flood Quantile Estimation.

Input Variables	Relative Importance, %		
	q10	q50	q100
Area	87.17	88.53	78.25
MBS	1.39	0.65	0.99
FAL	1.10	0.70	0.57
AMP	8.86	7.71	17.89
AMD	1.46	2.38	2.27

621

622

623

624

625

626

627

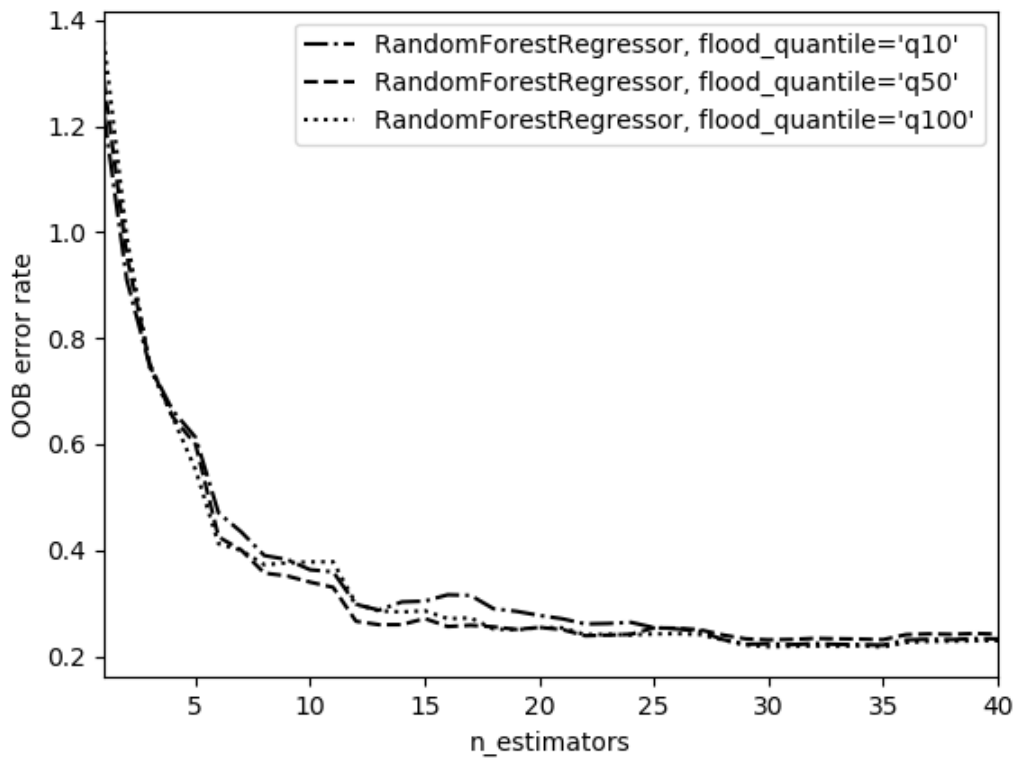
628

629

630

631



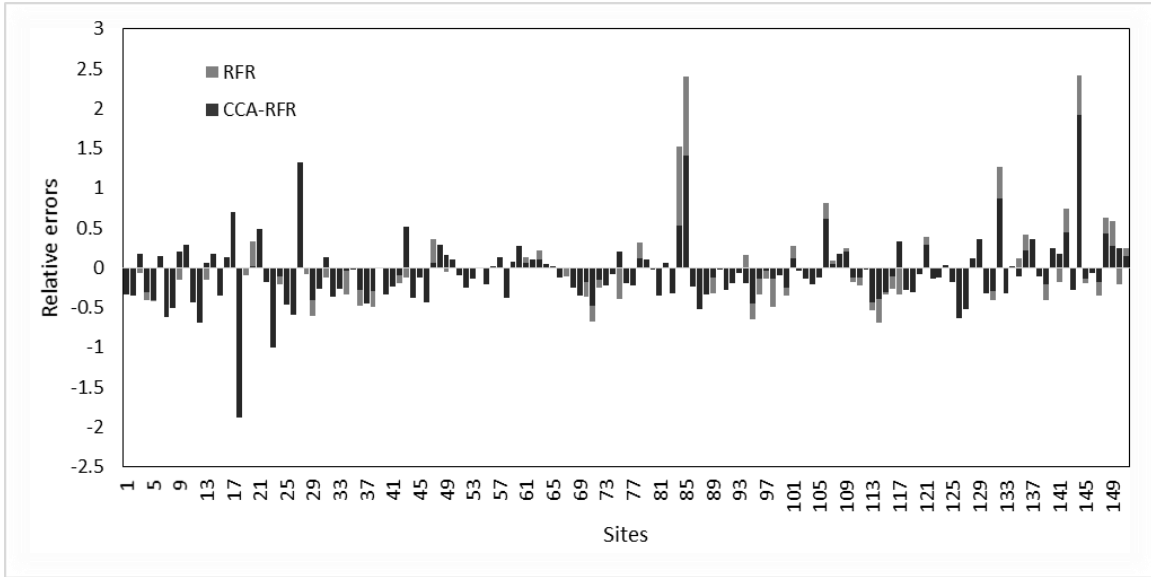


632

633 Figure 1: Number of trees (n\_estimators) vs OOB error rate for 10, 50 and 100-year flood quantiles.

634

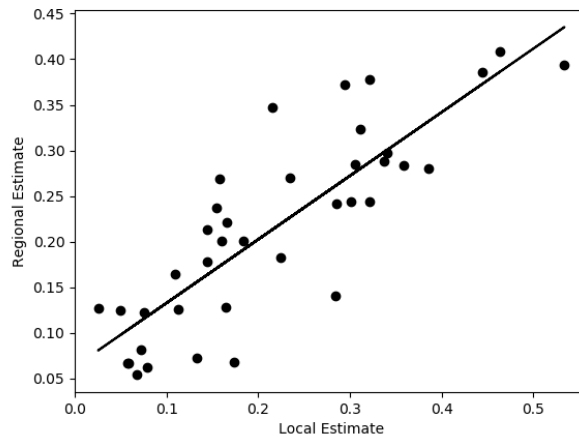
635



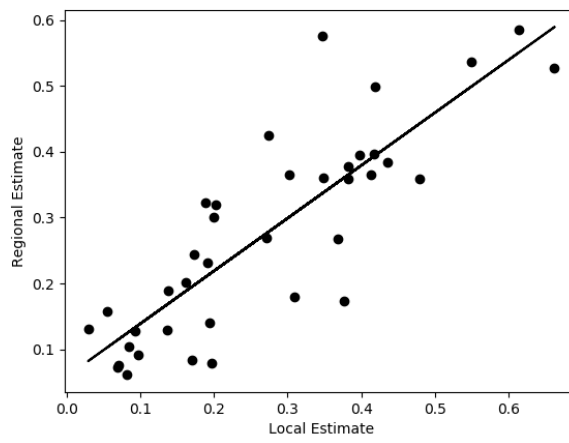
636

637 Figure 2: Relative errors associated with at-site quantiles  $q_{50}$  calculated using RFR and CCA-  
 638 RFR (the sites are ordered according to the increasing area)

A) q10 estimation



B) q50 estimation



C) q100 estimation

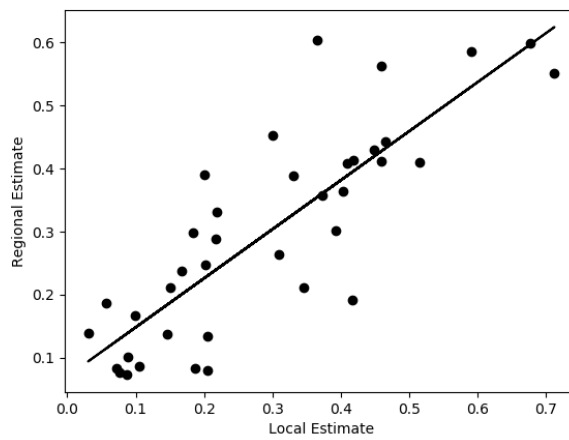
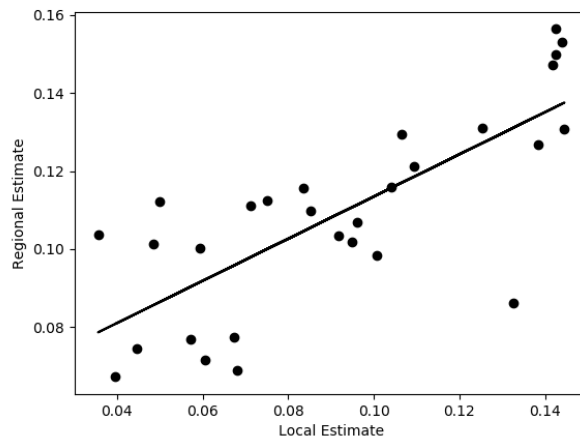
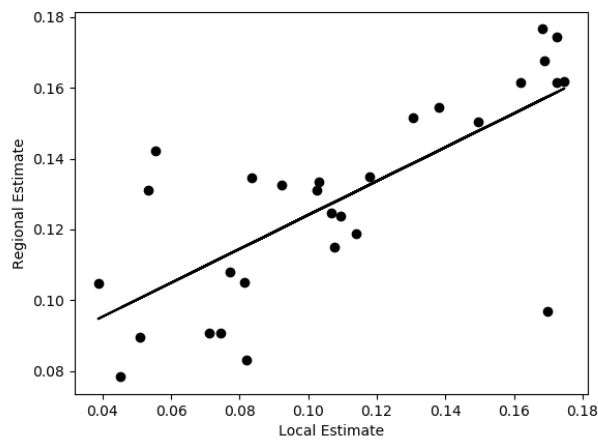


Figure 3: Estimation using the RFR approach

A) q10 estimation



B) q50 estimation



C) q100 estimation

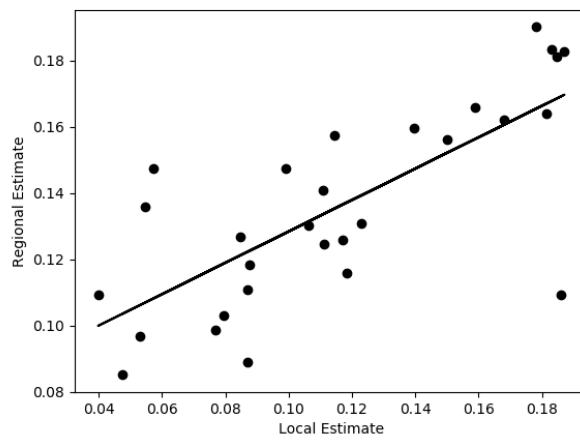


Figure 4: Estimation using the CCA-RFR approach